


Biomechanical Comparison of Krackow Repair and Percutaneous Achilles Repair System for Achilles Tendon Rupture Fixation: A Cadaveric and Finite Element Analysis Study

Bonnie Macaluso, MS^{1*}, Chaudhry R. Hassan, PhD^{1*} , David R. Swanson, MD², Alireza Nazemi, MD², Eugene Zaverukha, MS¹, Megan Paulus, MD², Yi-Xian Qin, PhD¹, and David E. Komatsu, PhD²

Abstract

Background: Open and percutaneous repair surgeries are widely used for the Achilles tendon rupture. However, prior biomechanic studies of these 2 approaches have mixed conclusions; therefore, we designed a cadaver and finite element (FE) model biomechanical study to compare the mechanical differences between the percutaneous Achilles repair system (PARS) and Krackow open repair under tensile load and rotation.

Methods: Sixteen Achilles tendons were extracted from fresh-frozen cadaver ankles and the calcaneums were fixed in mortar. A force control dynamic tensile mechanical test was performed at 1 Hz with 30- and 100-N cyclic loads. Initial intact baseline testing was followed by an incision on all Achilles tendons, 4 cm from the calcaneus insertion, which were then repaired using the PARS (n = 8) or Krackow (n = 8) method. Recorded force-displacement values were used to calculate mechanical parameters, and statistical significance of differences was determined by unpaired (between repair techniques) and paired (intact vs repaired) *t* tests. Material properties of the Achilles tendon in the FE model were modified and a 10-Nm flexion was simulated for intact and surgical groups.

Results: No differences were found between intact tendons assigned to PARS or Krackow repairs in Young's modulus ($P = .582$) and stiffness ($P = .323$). Pre- and postoperative Young's modulus was significantly decreased for both groups (Intact 230.60 ± 100.76 MPa vs PARS 142.44 ± 37.37 MPa, $P < .012$; Intact 207.46 ± 81.12 MPa vs Krackow 109.43 ± 27.63 MPa, $P < .002$). Stiffness decreased significantly after surgery for both groups (Intact 25.33 ± 10.89 N/mm vs PARS 6.51 ± 1.68 N/mm, $P < .003$; Intact 20.30 ± 8.65 N/mm vs Krackow 5.97 ± 1.30 N/mm, $P < .003$). PARS ultimate tensile strength was significantly higher than the Krackow (PARS 280.29 ± 47.32 N vs Krackow 196.97 ± 54.28 N, $P < .003$) but not significantly different in the ultimate tensile strain. PARS had a significantly lower postoperative gap compared to Krackow (PARS 9.75 ± 5.87 mm vs Krackow 25.19 ± 7.72 mm, $P < .001$). FE analysis predicted an increased talocalcaneal contact pressure, maximum principal stress, and rotation in the Krackow vs PARS models, respectively.

Conclusion: Biomechanical parameters observed in this study through mechanical testing and FE analysis favor the selection of PARS over the Krackow repair based on better strength, higher failure force, and lower gap generation.

Clinical Relevance: The study has analyzed two Achilles tendon repair methods using cadaver and numerical estimation and may help clinicians gain insight into selection of tendon repair approaches to generate better clinical outcomes.

Keywords: Achilles tendon, percutaneous tendon repair, Krackow repair, ankle finite element analysis, tendon biomechanics



Introduction

Acute rupture of the Achilles tendon is one of the most commonly reported tendon injuries in the United States with an incidence of 2.1 per 100 000 people per year,²⁵ the highest incidence in males aged 20-39 years (5.6/100 000) and a rising incidence in patients 40-59 years old.²¹ Injury to the Achilles tendon can lead to severe functional impairment and decreased quality of life. Numerous treatment methods have emerged over the last several decades in an effort to restore patients to their previous activities and avoid future disability. Despite a vast body of literature describing these methods, the ideal treatment for these injuries remains controversial.

Surgical repair of the Achilles tendon rupture can be performed in an open or percutaneous fashion. The most frequently described open techniques include the Krackow, Bunnell, and Kessler techniques^{9,14,15,25,27,32,33} with mixed biomechanical results reported when comparing these techniques.^{27,32} McCoy et al²⁷ concluded that the ultimate strength of the repair is based on the number of core suture strands crossing the repair site, not necessarily the pattern of the suture. The percutaneous repair technique was first described by Ma and Griffith in 1977²⁴ with numerous percutaneous repair techniques subsequently developed, including the Achillon, percutaneous Achilles repair system (PARS), and Tenolig system. Some biomechanical and clinical studies have demonstrated inferior results for percutaneous repair when compared to open techniques,^{15,25} whereas recent studies have shown that percutaneous techniques may provide equivalent or superior outcomes to open techniques.^{9,14} Evidence for the optimal treatment of acute Achilles tendon ruptures is conflicting both from an open and percutaneous perspective; however, as surgical techniques have evolved over the past few decades, there seems to be a shift in favor of percutaneous over open repair.^{17,33}

Young's modulus and stiffness of the tissues are important measures and data of the health of an Achilles tendon and strength of the repair.^{3,18} Calculating the material- and geometry-related properties of an Achilles tendon pre- and postrepair in conjunction with numerical predictions from finite element analysis (FEA) may provide insights for clinical procedure. To the authors' knowledge, this is the only biomechanical study specifically comparing the Krackow open repair technique with the PARS technique

using both cadaver measurements and FEA. FEA creates numerical predictions of biomechanical parameters within ankle joint space rotational loads and simulated tendon repairs that complement the cadaver-based biomechanical observations. Thus, the objective of this study is to provide concrete biomechanical data under physiological force and rotation loads for two of the most commonly used repair techniques to better inform clinical decisions and optimize patient outcomes.

Material and Methods

Cadaver Achilles Tendon

Patient demographics. Sixteen fresh-frozen cadaver ankles were used for Achilles tendon extraction. The samples were randomized into 2 different groups for surgical repair. The average ages were 68.50 and 69.00 years, the average weight was 71.44 and 78.36 kg, the average height was 173.36 and 173.69 cm, and BMI was 23.50 and 26.13 for PARS and Krackow groups, respectively. Mann-Whitney tests were performed on the patient data for the age, height, weight, and BMI to ensure that the groups were properly balanced and no significant differences were identified. (Supplementary Tables S1a and S1b).

Sample preparation. The Achilles tendons were extracted from the cadavers by transecting them at the origin of the gastrocnemius muscle and creating a coronal bone cut through the calcaneus approximately 2 inches anterior to the Achilles tendon insertion. The tendons were cleaned and adipose tissues were removed. The calcaneus bone segment was potted in a plastic mold and filled with mortar (Rapid Set Mortar Mix). Two Kirschner wires were transversally inserted to pin the bone in place and prevent slippage during loading. A machine screw was perpendicularly fixed at the bottom of the mold to attach to the mechanical testing system.

Loading procedure. A hydraulic, benchtop mechanical testing system (MTS 858 mini Bionix-II) was used in load control mode to replicate quasi-linear conditions and physical therapy exercises that are performed directly after the Achilles tendon surgery.^{9,30,32} The top of the tendon was secured in a custom clamp attached to the linear variable differential transformer (LVDT). The calcaneus potted end of the tendon was fixed to a 5000-N load cell.

¹Orthopaedic Bioengineering Research Laboratory, Department of Biomedical Engineering, Stony Brook University, Stony Brook, NY, USA

²Department of Orthopaedics, Stony Brook University Renaissance School of Medicine, Stony Brook, NY, USA

*Bonnie Macaluso, MS, and Chaudhry R. Hassan, PhD, contributed equally to this work and should be considered co-first authors.

Corresponding Author:

Yi-Xian Qin, PhD, Orthopaedic Bioengineering Research Laboratory, Department of Biomedical Engineering, Stony Brook University, Stony Brook, NY, USA
Email: Yi-Xian.Qin@stonybrook.edu

David E. Komatsu, PhD, Department of Orthopaedics, Stony Brook University Renaissance School of Medicine, Stony Brook, NY 11794-8434, USA
Email: david.komatsu@stonybrookmedicine.edu

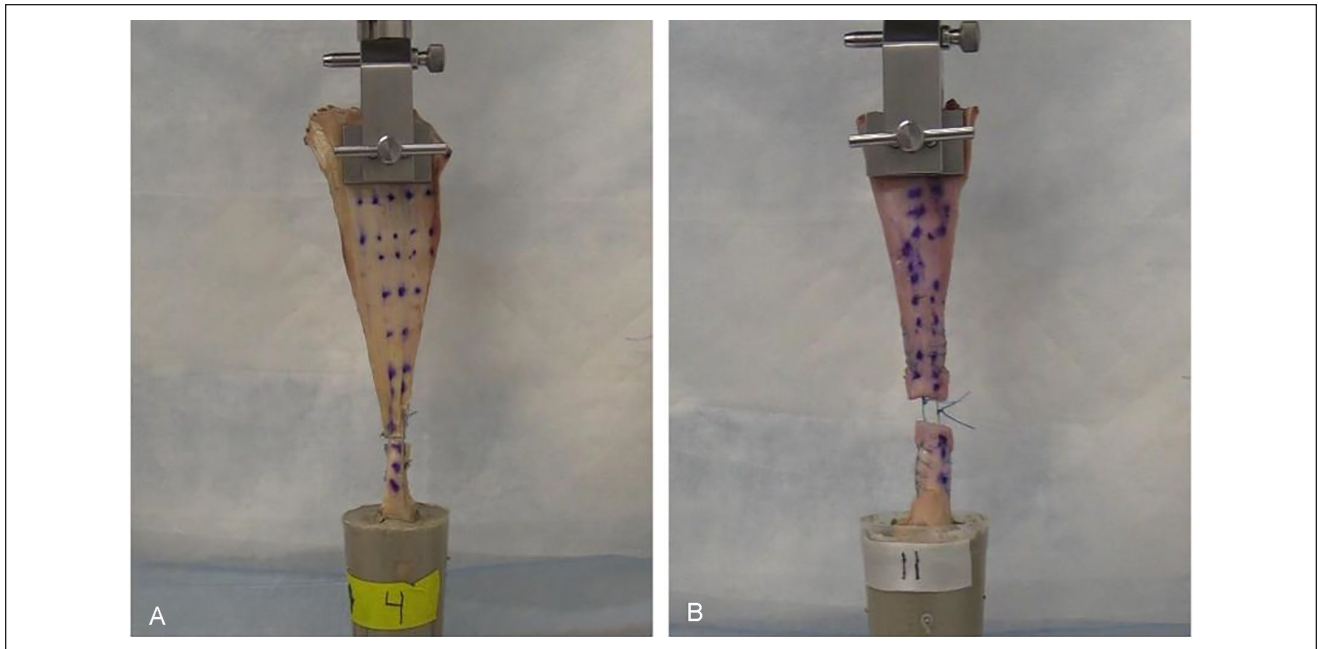


Figure 1. Mechanical testing setup with a custom-designed jig to hold the upper portion of the Achilles tendon. Calcaneus bone segment was fixed in mortar and attached to a load cell via a screw. (A) Percutaneous Achilles repair system (PARS) and (B) Krackow repaired tendons are shown here while under a tensile load of 100 N.

Tendons were periodically doused with saline during the duration of the loading to prevent drying. The cross-sectional area was measured at 4 and 9 cm from calcaneus insertion assuming a rectangular shape, and the smaller of the 2 measurements were recorded for use for stress-strain analysis. The following loading profiles were applied on the samples: (1) preload of 25 N for 5 minutes, (2) 5 to 30 N at 1 Hz for 30 cycles to precondition the tendons, (3) a ramp load to 100 N in 1 second, and (4) 25 to 100 N at 1 Hz for 500 cycles.

Surgical procedure. After initial intact testing, all Achilles tendon specimens were transected 4 cm proximal to the calcaneus insertion point. Subsequently, the tendons underwent surgical repair using either PARS or the Krackow method (Figure 1). The Krackow repair was created using a no. 2 FiberWire. We began in the portion of the tendon proximal to the repair site. The suture was introduced intra-substance at the repair site, and 5 running/locking loops were advanced through the tendon away from the repair site. The suture was then passed to the opposite side of the tendon, and 5 more running/locking loops were advanced back toward the repair site. This was repeated with another single no. 2 FiberWire suture in the portion of the tendon distal to the repair site. The sutures crossing the repair site were then tied together using 5 throws of a surgeon's knot. This configuration resulted in a total of 2 core strands traversing the repair site.

The PARS repair was created using the Arthrex PARS jig (Arthrex) using a set of color-coded sutures with 2 looped no. 2 FiberWire sutures as passing suture for the locking stitch and 3 SutureTape sutures as the repair sutures. We began with the portion of the tendon proximal to the repair site. The repair and passing sutures were passed through the jig in the standard, stepwise fashion. All sutures were then pulled down to the repair site using the jig. The 2 looped FiberWire passing sutures were used to lock the second (middle) SutureTape in the tendon, leaving a total of 6 core strands, 2 locking and 4 nonlocking. This sequence was repeated on the portion of the tendon distal to the repair site. Finally, all 6 core strands were tied together using 5 throws of a surgeon's knot.³³

The mechanical testing loading profile was then repeated with the addition of a 1-mm/s ramp displacement until ultimate failure as a final step. In addition, gapping was measured after 100 and 400 cycles for the postoperative groups, and a gap of more than 5 mm was considered a clinical failure; however, the tests were not stopped because of excessive gapping.

Data analysis and statistics. The force and displacement were measured from the mechanical tests at a sampling of 0.1 s. Stress, strain, and Young's modulus were determined from test values using a script written in MATLAB (Mathworks). Young's modulus was determined by linear curve fitting of stress-strain during the linear ramp loading to

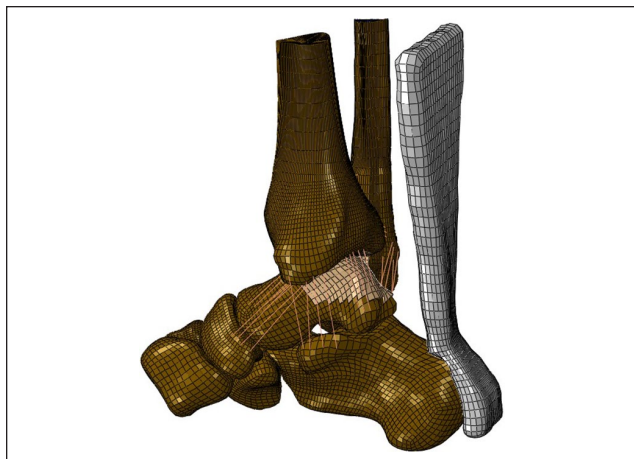


Figure 2. The complete finite element model with the bones of the ankle and the Achilles tendon. All tissues are modeled as hexahedral elements, except ligaments that are depicted as truss (wire) elements.

100 N. The ultimate tensile strain (%) and ultimate tensile stress (N/mm^2) were calculated from force and displacement data. The strain energy density was calculated as the area under the stress-strain curve. Paired (intact vs surgical groups) and unpaired (surgical group 1 vs group 2) Student t tests were used to compare groups, and values of $P < .05$ were considered statistically significant.

Finite Element Model Development

Model development. Ankle joint 3-dimensional bones geometry was obtained from a female patient computed tomography (CT) scan (Visible Human Project, University of Iowa, and National Institutes of Health) using image processing software MIMICS (Materialise). The Achilles tendon geometry was obtained from MRI scans (IRB exempt, sham and masked). Distal tibia and fibula, talus, calcaneus, navicular, cuboid, and cuneiform bones, and Achilles tendon were masked separately and meshed using IA-FEMesh (MIMX, University of Iowa) as 8-node hexahedral elements (Supplementary Table S6). Cartilage layers of approximately 1 mm were added to the tibia, fibula, talus, and calcaneus joint surfaces to create talofibular, talotibial, and talocalcaneal contacts.¹⁹ Eight ligaments were added using linear truss elements in Abaqus (v2016; Dassault Systemes) to represent posterior tibiofibular, anterior tibiofibular, calcaneofibular, and deltoid ligaments. The cross-sectional area for each element of the posterior tibiofibular, anterior tibiofibular, and other ligaments were 13, 22.98, and 110.3 mm^2 , respectively.^{6,12,23,28,29} The interosseous membrane was modeled using truss wire elements with a cross-sectional area of 20 mm^2 . The complete FE model is represented in Figure 2.

Table 1. Material properties for the intact and surgically repaired Achilles tendons.

Achilles Tendon Case	Young's Modulus (MPa)	Poisson Ratio
Intact	208	0.4
PARS	142	0.4
Krackow	109	0.4

Abbreviation: PARS, percutaneous Achilles repair system.

Material properties. All structures, except cartilage, were modeled as isotropic linear elastic materials. Cartilage tissue was modeled as neo-Hookean hyperelastic and viscoelastic material.⁵ Supplementary Tables S7a and S7b list material properties for all tissues except the Achilles tendon. The material properties of the Achilles tendon were determined through the above-mentioned mechanical testing and curve fitting the linear region of the stress-strain curve after preconditioning (Table 1). Linear elastic materials were assigned Young's modulus and Poisson ratio, which is a measure of tissue contraction under stretching or tissue expansion under compression.

Loading and boundary conditions. Surface-to-surface contacts were created for each of the cartilage joint surfaces between the bones (Supplementary Table S3). Small sliding was selected for all joints, except between the tibia-talus and fibula-tibia, which were modeled as finite sliding to avoid slippage and overclosure. The ligaments were attached to the appropriate body through a tie constraint. The model was validated under 600 N compressive load by comparing peak maximum contact stress and under 490 N compressive load by comparing contact area and location at talotibial joint surfaces, against published values from 2 studies.^{2,7} The loads were distributed 1:5 to the fibula and tibia, respectively, as an axial force applied on top of the segments. The distal surface of the cuneiforms and cuboid, as well as the bottom edge of the calcaneus, were fixed in all directions simulating a planted foot on a flat surface. The outer nodes of the tibia and fibula were fixed in the coronal and sagittal axis, relative to the loading axis. A 10-Nm pure moment was applied on the top of the tibia, fibula, and Achilles tendon segments to simulate ankle flexion. Analysis was repeated by changing Young's modulus of Achilles tendon corresponding to PARS and Krackow repairs.

Results

Cadaver Mechanical Test

Force, displacement, cross-sectional area, and length measurements were obtained from the tensile mechanical testing of the Achilles tendons to calculate mechanical

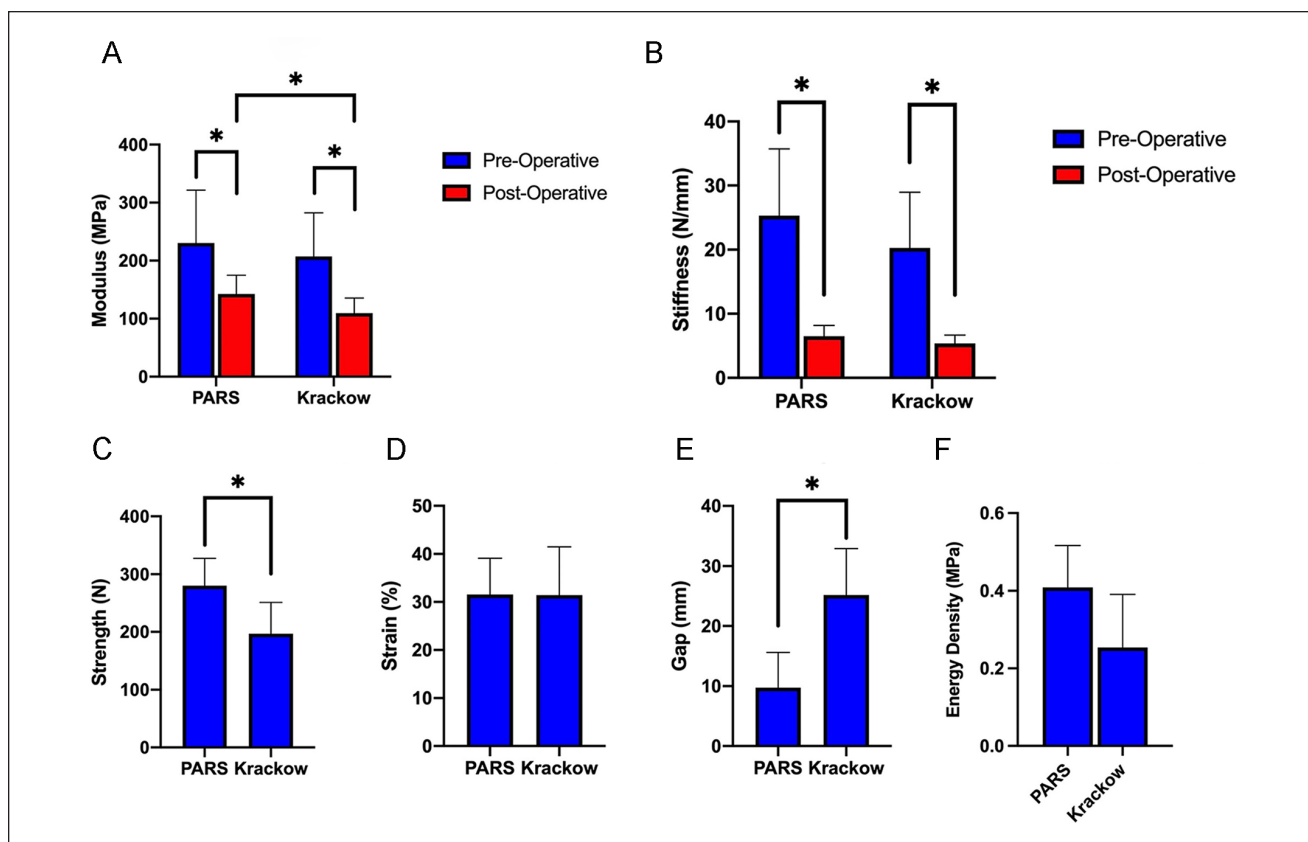


Figure 3. Mechanical parameters calculated from tensile loading of the cadaver Achilles tendon. (A) Young’s modulus; (B) stiffness; (C) ultimate tensile strength; (D) ultimate tensile strain; (E) gap between the Achilles tendon sutured segments after 400 cycles; and (F) strain energy density. (A)-(D) and (F) were determined from force, displacement, cross-sectional area, and length measurements of the Achilles tendon.

parameters for comparison between groups (Figure 3 and Supplementary Table S2). There were no significant differences in Young’s modulus ($P = .582$) and stiffness ($P = .323$) between the 2 preoperative intact groups. A significant difference in pre- and postoperative Young’s modulus was found for both groups. The average preoperative Young’s modulus for PARS group was 230.60 ± 100.76 MPa for intact tendon, which decreased to 142.44 ± 37.37 MPa postoperatively ($P < .012$). Similarly, the preoperative Young’s modulus for the intact Krackow group was 207.46 ± 81.12 MPa, which decreased to 109.43 ± 27.63 MPa postoperation ($P < .002$). Additionally, there was a significant difference between both postoperative groups ($P < .021$). The average stiffness for preoperative PARS and Krackow groups was 25.33 ± 10.89 and 20.30 ± 8.65 N/mm ($P = .323$ between preoperative groups), respectively, which decreased postoperatively to 6.51 ± 1.68 N/mm ($P < .003$) and 5.97 ± 1.30 N/mm ($P < .003$), respectively, for PARS and Krackow groups. Postoperatively, there was no significant difference between the stiffness of both groups ($P = .485$).

The ultimate tensile strength (UTS) for the PARS group was 280.29 ± 47.32 N, which was significantly higher than

196.97 ± 54.28 N for the Krackow group ($P < .003$). The ultimate tensile strain was 31.55 ± 7.54 and 31.42 ± 10.05 for postoperative PARS and Krackow groups, respectively, and was not significantly different ($P = .977$). The method of failure was observed to be different for PARS and Krackow groups: PARS failure occurred predominantly as suture ripping out from the tissue, whereas Krackow failure was the breaking of at least 1 suture. The gapping length was significantly lower ($P < .001$) after 400 cycles for the PARS group (9.75 ± 5.87 mm) compared to the Krackow group (25.19 ± 7.72 mm). Moreover, strain energy density when ramping the load from 25 to 100 N was found to be different between the postoperative groups but without statistical significance ($P = .056$): 0.409 ± 0.108 vs 0.254 ± 0.137 MPa for PARS and Krackow, respectively.

Finite Element Model Validation

Figure 4 shows a 2-dimensional von Mises stress contour plot under a 600-N axial force. Tibial cartilage computed values ranged between 1.02 and 3.34 MPa, whereas talar cartilage estimated stress values ranged between 0.85 and

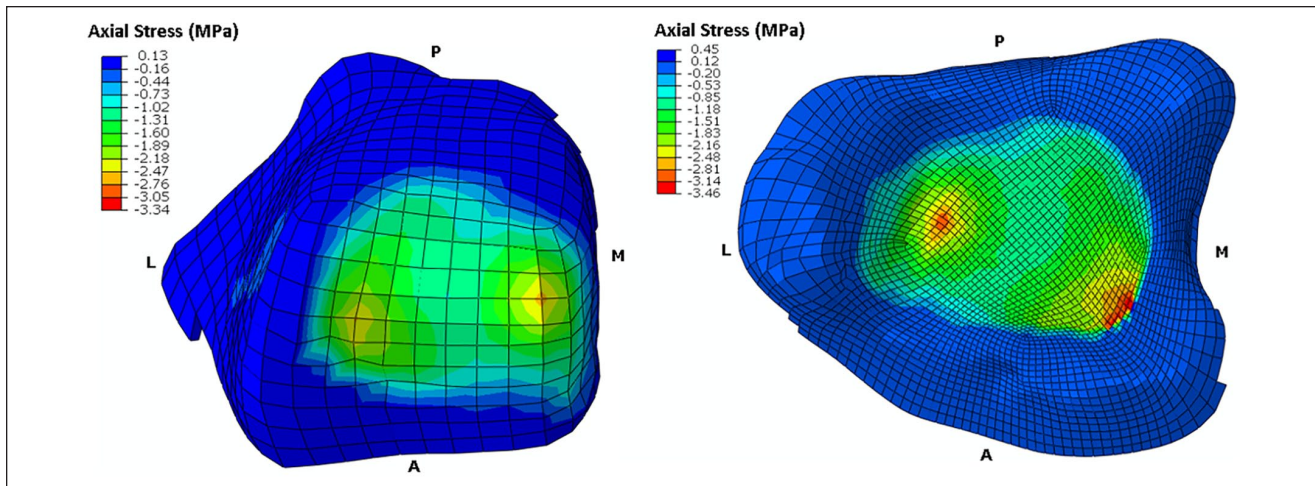


Figure 4. Estimated von Mises stress on the tibiotalar cartilage for superior side of talus (left) and inferior side tibia (right) under a 600 N load.

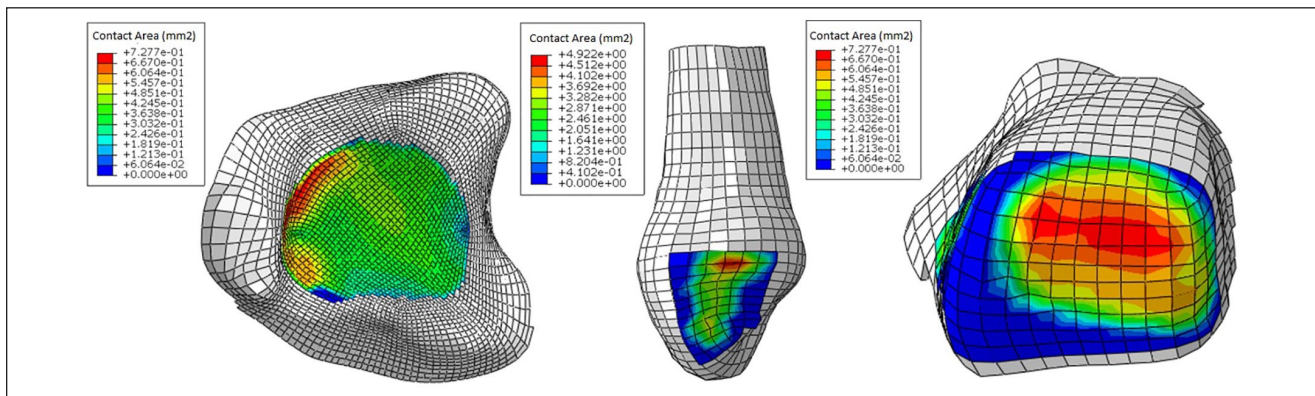


Figure 5. Contact area made by surface nodes of the tibiotalar and fibulotalar joints under 490 N compressive force. Maximum predicted contact area in the tibiotalar joint was 0.728 mm^2 .

3.46 MPa, which aligned with the reported values from Anderson et al (1.5-4 MPa).² Maximum stress concentrations were skewed medially for both talus and tibia, and a maximum point was located in the medial posterior corner on the tibial cartilage. Predicted stress distribution agreed with published cadaver studies, which reported tibiotalar contact stress values between 1.4 and 4.0 MPa.² Figure 5 represents a 2-dimensional contact area plot under the 490-N axial force. The stress was concentrated on the medial side and on the superior side of the talotibial cartilage with a range of 0.34 to 4.10 MPa; this distribution was similar to the one reported by Calhoun et al⁷ in their ankle joint cadaver test under the same load.

Mechanical Parameter Prediction Under Rotational Load

Under the 10-Nm flexion moment, the ankle joint rotated with the distal calcaneus region fixed. The healthy ankle

joint rotated by 2.57 degrees, which increased to 2.84 and 3.02 degrees for PARS and Krackow simulated surgical models, respectively. Achilles tendon maximum principal stress under flexion was predicted (Supplementary Table S4) as 3.05 MPa for the healthy, which increased to 3.18 and 3.36 MPa for PARS and Krackow models, respectively. Similarly, the maximum principal stress in the calcaneus was 2.71 MPa for the healthy case, which increased to 2.97 and 3.10 MPa for PARS and Krackow models, respectively. Lastly, talus maximum principal stress was predicted as 1.70 MPa for the healthy, which increased to 1.73 and 1.74 MPa for PARS and Krackow, respectively. The maximum principal strain on the Achilles tendon was predicted to be 0.013 for the healthy case, which increased to 0.0197 and 0.0258 for PARS and Krackow, respectively. Tibial distal cartilage surface in contact with talus had maximum predicted contact pressure (Supplementary Table S5) of 1.59, 1.61, and 1.60 MPa for the healthy, PARS, and Krackow cases, respectively. Talus proximal

cartilage surface in contact with tibial had predicted maximum contact pressure of 1.31, 1.33, and 1.33 MPa for the healthy, PARS, and Krackow cases, respectively. Talus distal cartilage surface in contact with calcaneus had predicted maximum contact pressure of 1.76, 1.78, and 1.80 MPa for the healthy, PARS, and Krackow cases, respectively. Calcaneus cartilage proximal surface in contact with the talus had predicted maximum contact pressure of 1.62, 1.64, and 1.66 MPa for the healthy, PARS, and Krackow cases, respectively.

Discussion

The principal goal of this study was to evaluate and compare 2 of the most commonly used techniques for repairing Achilles tendon ruptures: the PARS percutaneous technique and the open Krackow repair. PARS repair has been reported to have a low rate of complications, improved cosmetic appearance,²² higher American Orthopaedic Foot & Ankle Society (AOFAS) ankle-hind-foot score, decreased operation time,³³ and faster recovery times¹¹ when compared to open repair techniques. One of the primary outcome measures of the cadaver study was the gapping at the repair site. We noted a significant decrease in repair gapping for the minimally invasive PARS compared to the Krackow open surgery at both the 100th cycle (2.6 and 4.8 mm, respectively) and 400th cycle (9.8 and 25.2 mm, respectively). Repair gapping can have detrimental effects on strength and function following surgery.²⁶ Open Krackow repair, although known to have excellent pullout resistance, has been shown to have decreased resistance to gap formation.⁴ Some prior studies evaluating gap formation have used a surrogate marker with initial linear stiffness.^{10,14} Contrary to these studies, we presume direct measurement to be a more accurate assessment of repair site gapping. To the authors' knowledge, there is only 1 existing biomechanical study to date to directly measure tendon gapping without the use of a surrogate.⁹ These authors demonstrated significantly lower early elongation with open repair as opposed to various percutaneous techniques. Our study directly measured gap formation without using a surrogate marker and provides contrasting data to the study by Clanton et al,⁹ suggesting that the PARS technique has a higher resistance to gap formation than open repair. Techniques such as epitendinous suture, gift-box technique, and double suture weave have been shown to decrease tendon gapping with open repair.^{1,26} However, controlled clinical studies need to be performed to verify the clinical significance of these differences and determine whether the suggested modifications can provide superior gap resistance to percutaneous techniques.

Mechanical strength of the repair was another primary outcome of the cadaver mechanical testing, which was measured as an increased load to failure for the PARS compared to the Krackow (280.29 and 196.97 N, respectively). Tensile strength is of particular importance to the quality of the repair and the subsequent ability of the tendon to heal in the postoperative period. Heitman et al¹⁴ used the percutaneous Achillon system and, similar to our results, found higher load to failure and work to failure for percutaneous repair over the open Krackow technique. Moreover, they found that the predominant method of repair failure was suture break for Krackow open repair and suture tearing through the tissue for percutaneous repair, which are consistent with our observations. Similarly, Huffard et al¹⁶ found increased load to failure (276 and 342 N) when comparing the Krackow and Achillon methods, respectively. Akizuki et al described the forces on the Achilles tendon to range from 191 N (immobilized 1-inch heel lift) to 555 N (walking) under 4 different walking conditions during postoperative rehabilitation.¹ Based on the published force values, PARS repair should remain intact under low force activities during the rehabilitation process, whereas Krackow repair would likely rupture under even low force activity of heel lift.¹ However, these differences in UTS are not consistent with some previously published biomechanical studies.^{9,10} Clanton et al⁹ compared 4 variations of Achilles repair surgeries: open repair, the Achillon System, the PARS System, and an Achilles Midsubstance SpeedBridge. They reported no significant difference in the UTS of repair between the open and percutaneous methods. However, they did not precondition the tendons at the start of the *in vitro* mechanical test that is often used as a way to mimic warmup exercises patients would endure prior to engaging in physical therapy.¹³ In addition, preconditioning allows for the soft tissues being studied to achieve a steady state prior to biomechanical testing⁸ and standardizes the comparison between the different specimens because of the visco-hyperelastic nature of tendons.¹⁰ Dekker et al¹⁰ found that the Krackow method exhibited a significantly increased initial stiffness over the PARS method and no significant difference in the average load and failure between the 2 methods. However, despite their results, they concluded that the PARS system should be favored due to the comparable biomechanics and limited damage to surrounding soft tissue. Moreover, they found the locations of repair failure to align with Heitman et al¹⁴ and our study, with Krackow failing at the sutures and PARS failing at the tissue suture interface. We believe regardless of the inconsistency in biomechanical findings in previous literature comparing minimally invasive and open repairs that our results could indicate that the minimally invasive PARS technique provides a biomechanical environment that may translate to

improved short- and long-term clinical outcomes. This conclusion is strengthened by the results of our finite element simulations.

Young's modulus is the intrinsic material property that is determined by the stress over strain in a unidirectional load and is independent of specimen geometry. Stiffness depends on the geometry of the specimen, its shape, and the boundary conditions of the loading profile. Because of our uniaxial loading conditions, the stiffness is directly proportional to the Young's modulus of the tendon. Young's modulus and stiffness are important measures of the health of an Achilles tendon and strength of the repair^{3,18,20} and was another primary outcome of our testing. Kawakami et al¹⁸ reported a positive correlation between the Achilles tendon stiffness and ankle plantar flexion torque and concluded that 70% of ankle joint torque is due to variations in the Achilles tendon stiffness. Additionally, their study found a correlation between the Achilles tendon stiffness and foot plantar pressure, which indicated that the tendon stiffness plays a role in the force transmission through the ankle to the foot. A decrease in the Achilles tendon stiffness is also shown to shorten muscle fascicles, which creates a change in gait and biomechanics of the ankle.³ Our study found that the PARS group has higher postrepair Young's modulus compared to the Krackow group. Based on the above-mentioned studies, our results suggest that the PARS repair would have favorable clinical outcome compared to Krackow repair.

When a 10-Nm flexion moment was applied to the intact, Krackow, and PARS models, the maximum predicted principal stress on the Achilles tendon, calcaneus, and talus increased in the Krackow compared to PARS based models. Similarly, the maximum tensile strain on the Achilles tendon, contact pressure at the talocalcaneal joint, and degrees of rotation were elevated for the Krackow compared to the PARS model. Sun et al³¹ found an increased ankle dorsiflexion angle, increased loading rate, and decreased knee flexion 18-24 months after surgical repair of Achilles tendon rupture, with the most likely reason being the tendon elongation. These findings correspond with variations in gait, ankle torque, and plantar pressure due to decreased stiffness of the Achilles tendon and agrees with our FEA-predicted increased maximum stresses and degrees of rotation. Moreover, the location and changes of the stresses and pressure on the cartilage in the tibiotalar joint point to a differing force translation and distribution. This suggests that PARS repair may be more resistant to long-term Achilles tendon elongation and the biomechanical effects of decreased stiffness. The authors conclude that this change in gait can lead to an increased risk of injury,

namely, tibial stress fractures, and ankle sprain long after postoperative rehabilitation.

The current study has some limitations in the design and subsequent experiments. The cadaver study used tendon samples from White donors only, and all but 1 were male. There is a known difference in the material properties of the Achilles tendon between females and males; however, Achilles tendon ruptures are more common in males. Additionally, the open Krackow and PARS repairs were performed using direct visualization in the entire Achilles tendon. This introduces the benefit of seeing directly where the sutures are passing through the tendon in the PARS technique. The surgeries were performed as a time zero repair with the tendon tears induced as clean transections that do not exactly mimic the often-frayed edges of torn tendon seen clinically. Additionally, the average age of the donor tendons in this study was 66 years, whereas the average age group for Achilles tendon ruptures is 40-49 years. The cadaver test was performed without any surrounding soft tissues and, therefore, does not exactly represent the actual in vivo surgical environment. The knots from PARS repair are not always directly on the tendon, which can cause them to loosen in actual practice. The FE model was based on a geometry of a female lower extremity and foot, whereas the Achilles tendon geometry was obtained from one of the male cadaver ankles. FEA used a single source of ankle and foot geometry to perform the biomechanical estimation analysis, which requires setting up of a future cadaver or clinical study to determine the biomechanical effects on the ankle joint after the Achilles tendon repair under compressive and rotational loads. Finally, the FE model only simulated flexion motion, which can be enhanced in future studies with adduction and abduction motions with in vitro and clinical validation.

In conclusion, the results of this study provide biomechanical data to assist in the management of Achilles tendon tears with different approaches to treatment. The ability to apply data to this decision, such as tendon gapping, UTS, increased stresses, and rotations in the joints of the ankle, will better inform those involved in the decision-making process. Ultimately, the decision to perform surgery and which technique to implement may be dictated by the surgeon level of comfort and experience and patient preference. The findings of this study can be further enhanced in future researches, such as a randomized controlled trial comparing the open Krackow technique to PARS repair, postoperative strain, and gap analysis using image processing on the video footage, and performing extensive FE analysis to determine the localization of stress and strain in the tissues of the ankle joint, which will help in better understanding the effectiveness and limitations of these procedures.

Supplementary Table 1a. Patient demographics of PARS group.

Ankle	Age	Race	Sex	Height(cm)	Weight(kg)	BMI
R	69	C	M	182.9	99.8	30
L	53	C	M	182.9	72.6	22
L	70	C	F	154.9	36.3	15
R	72	C	M	165.1	56.7	21
L	68	C	M	167.6	77.1	27
L	71	C	M	182.9	77.1	23
R	69	C	M	182.9	79.4	24
L	76	C	M	167.6	72.6	26

Supplementary Table 1b. Patient demographics of Krackow group.

Ankle	Age	Race	Sex	Height(cm)	Weight(kg)	BMI
L	68	C	M	172.7	103.4	35
L	81	C	M	177.8	80.7	26
R	53	C	M	182.9	72.6	22
L	72	C	M	165.1	56.7	21
R	68	C	M	167.6	77.1	27
R	71	C	M	182.9	77.1	23
L	69	C	M	182.9	79.4	24
R	69	C	M	167.6	72.6	26

Supplementary Table 2. Comparison of results between PARS and Krackow groups.

Parameter	PARS	Krackow
Ultimate Tensile Strain (%)	31.55	31.42
Ultimate Tensile Strength (N)**	280.29	196.97
Young's Modulus (MPa)**	142.44	109.43
Stiffness (N/mm)	6.51	5.97
Gapping (100c)(mm)**	2.56	4.78
Gapping (400c)(mm)**	9.75	25.19
Parameter	Intact Group 1	Intact Group 2
Young's Modulus (MPa)	230.60	207.15
Stiffness (N/mm)	25.33	20.30
P value Between Intact and Surgical Group	Young's Modulus = 0.020 Stiffness = 0.003	Young's Modulus = 0.001 Stiffness = 0.002

**P value < 0.05 between groups.

Supplementary Table 3. Interaction Properties for Surface to Surface Contacts

Bodies	Friction Coefficient	P0 (MPa)	d0 (mm)	Clearance (mm)
Tibia-Talus	0.02	6	0.4	-
Fibula-Tibia	0.02	4	0.4	-
Talus-Anterior Calcaneus	0.02	10	2	3
Talus-Posterior Calcaneus	0.02	10	2	2
Talus- Navicular	0.02	10	0.5	0.495
Navicular- Cuneiforms	0.02	10	1	0.95
Calcaneus- Cuboid	0.02	10	2.2	2.15

Supplementary Table 4. Predicted maximum principal stress in the tissues of Achilles tendon, Calcaneus, and Talus under 10 Nm flexion moment.

Maximum Principal Stress (MPa)	Achilles Tendon	Calcaneus	Talus
Intact	3.05	2.71	1.70
PARS	3.18	2.97	1.73
Krakow	3.36	3.10	1.74

Supplementary Table 5. Predicted maximum contact pressure in the tibio-talar and talo-calcaneus joints under 10 Nm flexion moment.

Maximum Contact Pressure (MPa)	Tibial Distal Surface	Talar Proximal Surface	Talus Distal Surface	Calcaneus Proximal Surface
Intact	1.59	1.31	1.76	1.62
PARS	1.61	1.33	1.78	1.64
Krakow	1.60	1.33	1.80	1.66

Supplementary Table 6. Finite element mesh details for each tissue of the ankle joint bones, ligaments, and tendon.

Tissue	Average Area (mm ²)	Number of elements
Tibia	0.8 × 1.5	164691
Fibula	1.8 × 3.1	33200
Talus	1.9 × 2.3	4227
Calcaneus	1.9 × 2.6	6400
Navicular	1.5 × 2.0	2000
Cuneiforms	1.3 × 1.9	5592
Cuboid	2.0 × 2.8	1280
Achilles Tendon		3600
Ligaments	NA	42
Interosseous Membrane	NA	4

Supplementary Table 7a. Material properties of isotropic, linear elastic tissues.

Tissue	Young's Modulus (MPa)	Poisson's Ratio
Cortical Bone	12000	0.3
Trabecular Bone	800	0.3
Interosseous Membrane	260	0.4
Anterior Talo-fibular Ligament	255.5	0.49
Posterior Talo-fibular Ligament	216.5	0.49
Other Ligaments	250	0.49

Supplementary Table 7b. Material properties for the cartilage.

Hyperelastic		
C10	D1	
0.176	0.96	
Viscoelastic		
G _i Prony	K _i Prony	τ _i Prony
0.73	0	10
0.03	0	100
0.232	0	1000

Ethical Approval

Ethical approval for this study was waived by the Stony Brook University Institutional Review board because no aspects of the study are considered human subjects research.

Declaration of Conflicting Interests

The author(s) declared no potential conflicts of interest with respect to the research, authorship, and/or publication of this article. ICMJE forms for all authors are available online.

Funding

The author(s) disclosed receipt of the following financial support for the research, authorship, and/or publication of this article: National Institutes of Health (R01AR61821, YXQ), and National Space Biomedical Research Institute (SMST03401, YXQ).

ORCID iD

Chaudhry R. Hassan, PhD,  <https://orcid.org/0000-0001-6596-9603>

References

1. Akizuki K, Gartman E, Nisonson B, Ben-Avi S, McHugh M. The relative stress on the Achilles tendon during ambulation in an ankle immobiliser: implications for rehabilitation after Achilles tendon repair. *Br J Sports Med.* 2001;35(5):329-333.
2. Anderson DD, Goldsworthy JK, Li W, Rudert MJ, Tochigi Y, Brown TD. Physical validation of a patient-specific contact finite element model of the ankle. *J Biomech.* 2007; 40(8):1662-1669.
3. Arya S, Kulig K. Tendinopathy alters mechanical and material properties of the Achilles tendon. *J Appl Physiol.* 2010; 108(3):670-675.doi:10.1152/jappphysiol.00259.2009
4. Barmakian JT, Lin H, Green SM, Posner MA, Casar RS. Comparison of a suture technique with the modified Kessler method: resistance to gap formation. *J Hand Surg.* 1994;19(5):777-781.
5. Braito M, Dammerer D, Reinthaler A, Kaufmann G, Huber D, Biedermann R. Effect of coronal and sagittal alignment on outcome after mobile-bearing total ankle replacement. *Foot Ankle Int.* 2015;36(9):1029-1037.

6. Burstein AH, Reilly DT, Martens M. Aging of bone tissue: mechanical properties. *J Bone Joint Surg Am.* 1976;58(1):82-86.
7. Calhoun JH, Li F, Ledbetter BR, Viegas SF. A comprehensive study of pressure distribution in the ankle joint with inversion and eversion. *Foot Ankle Int.* 1994;15(3):125-133.
8. Cheng S, Clarke EC, Bilston LE. The effects of preconditioning strain on measured tissue properties. *J Biomech.* 2009;42(9):1360-1362.
9. Clanton TO, Haytmanek CT, Williams BT, et al. A biomechanical comparison of an open repair and 3 minimally invasive percutaneous Achilles tendon repair techniques during a simulated, progressive rehabilitation protocol. *Am J Sports Med.* 2015;43(8):1957-1964.
10. Dekker RG, Qin C, Lawton C, et al. A biomechanical comparison of limited open versus Krackow repair for Achilles tendon rupture. *Foot Ankle Orthop.* 2017;2(4):2473011417715431.
11. Gigante A, Moschini A, Verdenelli A, Del Torto M, Ulisse S, De Palma L. Open versus percutaneous repair in the treatment of acute Achilles tendon rupture: a randomized prospective study. *Knee Surg Sports Traumatol Arthrosc.* 2008;16(2):204-209.
12. Golanó P, Vega J, de Leeuw PA, et al. Anatomy of the ankle ligaments: a pictorial essay. *Knee Surg Sports Traumatol Arthrosc.* 2010;18(5):557-569. doi:10.1007/s00167-010-1100-x
13. Hawkins D, Lum C, Gaydos D, Dunning R. Dynamic creep and pre-conditioning of the Achilles tendon in-vivo. *J Biomech.* 2009;42(16):2813-2817.
14. Heitman DE, Ng K, Crivello KM, Gallina J. Biomechanical comparison of the Achillon® tendon repair system and the Krackow locking loop technique. *Foot Ankle Int.* 2011;32(9):879-887.
15. Hockenbury RT, Johns JC. A biomechanical in vitro comparison of open versus percutaneous repair of tendon Achilles. *Foot Ankle.* 1990;11(2):67-72.
16. Huffard B, O'Loughlin P, Wright T, Deland J, Kennedy J. Achilles tendon repair: Achillon system vs. Krackow suture: an anatomic in vitro biomechanical study. *Clin Biomech.* 2008;23(9):1158-1164.
17. Karabinas PK, Benetos IS, Lampropoulou-Adamidou K, Romoudis P, Mavrogenis AF, Vlamis J. Percutaneous versus open repair of acute Achilles tendon ruptures. *Eur J Orthop Surg Traumatol.* 2014;24(4):607-613. doi:10.1007/s00590-013-1350-7
18. Kawakami Y, Kanehisa H, Fukunaga T. The relationship between passive ankle plantar flexion joint torque and gastrocnemius muscle and Achilles tendon stiffness: implications for flexibility. *J Orthop Sports Phys Ther.* 2008;38(5):269-276. doi:10.2519/jospt.2008.2632
19. Kazemi M, Li L. A viscoelastic poromechanical model of the knee joint in large compression. *Med Eng Phys.* 2014;36(8):998-1006.
20. Laurent D, Walsh L, Muaremi A, et al. Relationship between tendon structure, stiffness, gait patterns and patient reported outcomes during the early stages of recovery after an Achilles tendon rupture. *Sci Rep.* 2020;10(1):20757. doi:10.1038/s41598-020-77691-x
21. Lemme NJ, Li NY, DeFroda SF, Kleiner J, Owens BD. Epidemiology of Achilles tendon ruptures in the United States: athletic and nonathletic injuries from 2012 to 2016. *Orthop J Sports Med.* 2018;6(11):2325967118808238.
22. Lim J, Dalai R, Waseem M. Percutaneous vs. open repair of the ruptured Achilles tendon—a prospective randomized controlled study. *Foot Ankle Int.* 2001;22(7):559-568.
23. Linde F, Hvid I, Pongsoipetch B. Energy absorptive properties of human trabecular bone specimens during axial compression. *J Orthop Res.* 1989;7(3):432-439.
24. Ma G, Griffith TG. Percutaneous repair of acute closed ruptured Achilles tendon: a new technique. *Clin Orthop Relat Res.* 1977(128):247-255.
25. Manent A, Lopez L, Vilanova J, et al. Assessment of the resistance of several suture techniques in human cadaver Achilles tendons. *J Foot Ankle Surg.* 2017;56(5):954-959.
26. Maquirriain J. Achilles tendon rupture: avoiding tendon lengthening during surgical repair and rehabilitation. *Yale J Biol Med.* 2011;84(3):289.
27. McCoy BW, Haddad SL. The strength of Achilles tendon repair: a comparison of three suture techniques in human cadaver tendons. *Foot Ankle Int.* 2010;31(8):701-705.
28. Mondal S, Ghosh R. A numerical study on stress distribution across the ankle joint: Effects of material distribution of bone, muscle force and ligaments. *J Orthop.* 2017;14(3):329-335.
29. Siegler S, Block J, Schneck CD. The mechanical characteristics of the collateral ligaments of the human ankle joint. *Foot Ankle.* 1988;8(5):234-242.
30. Soroceanu A, Sidhwa F, Aarabi S, Kaufman A, Glazebrook M. Surgical versus nonsurgical treatment of acute Achilles tendon rupture: a meta-analysis of randomized trials. *J Bone Joint Surg Am.* 2012;94(23):2136.
31. Sun D, Fekete G, Mei Q, Gu Y. Gait abnormality and asymmetry analysis after 18–24 months surgical repair of unilateral Achilles tendon rupture. *J Med Imag Health Inform.* 2019;9(3):552-560.
32. Watson TW, Jurist KA, Yang KH, Shen KL. The strength of Achilles tendon repair: an in vitro study of the biomechanical behavior in human cadaver tendons. *Foot Ankle Int.* 1995;16(4):191-195.
33. Yang B, Liu Y, Kan S, et al. Outcomes and complications of percutaneous versus open repair of acute Achilles tendon rupture: a meta-analysis. *Int J Surg.* 2017;40:178-186.